

Impedance Control Balances Stability With Metabolically Costly Muscle Activation

David W. Franklin,^{1,3} Udell So,² Mitsuo Kawato,¹ and Theodore E. Milner³

¹ATR Computational Neuroscience Laboratories and ²ATR Human Information Science Laboratories, Keihanna Science City, Kyoto 619–0288, Japan; and ³School of Kinesiology, Simon Fraser University, Burnaby, British Columbia V5A 1S6, Canada

Submitted 9 April 2004; accepted in final form 9 June 2004

Franklin, David W., Udell So, Mitsuo Kawato, and Theodore E. Milner. Impedance control balances stability with metabolically costly muscle activation. *J Neurophysiol* 92: 3097–3105, 2004. First published June 16, 2004; 10.1152/jn.00364.2004. Humans are able to stabilize their movements in environments with unstable dynamics by selectively modifying arm impedance independently of force and torque. We further investigated adaptation to unstable dynamics to determine whether the CNS maintains a constant overall level of stability as the instability of the environmental dynamics is varied. Subjects performed reaching movements in unstable force fields of varying strength, generated by a robotic manipulator. Although the force fields disrupted the initial movements, subjects were able to adapt to the novel dynamics and learned to produce straight trajectories. After adaptation, the endpoint stiffness of the arm was measured at the midpoint of the movement. The stiffness had been selectively modified in the direction of the instability. The stiffness in the stable direction was relatively unchanged from that measured during movements in a null force field prior to exposure to the unstable force field. This impedance modification was achieved without changes in force and torque. The overall stiffness of the arm and environment in the direction of instability was adapted to the force field strength such that it remained equivalent to that of the null force field. This suggests that the CNS attempts both to maintain a minimum level of stability and minimize energy expenditure.

INTRODUCTION

Humans constantly interact with their environment in everyday life. For example, to drink from a cup, a person must successfully reach for the cup, pick it up, and bring it to his/her mouth without spilling the contents. To successfully complete this activity, the person must be able to compensate for the forces exerted on the arm by the movement of the cup and its contents. It is widely accepted that the human CNS learns about the dynamics of the physical world, and in particular, learns to compensate for externally imposed forces on the arm during movements (Conditt et al. 1997; Krakauer et al. 1999; Lackner and Dizio 1994; Shadmehr and Mussa-Ivaldi 1994).

Previous studies have provided evidence that the CNS learns an internal model of the interaction dynamics when movements are performed in novel mechanical environments (Kawato 1999). That is, the CNS obtains a neural representation of the relationship between motor command and actual movement. However, these studies focused primarily on stable interactions with the environment.

Relatively few studies have investigated adaptation to unstable interactions. Unstable interactions are as important as

stable interactions since they routinely occur in daily activities that involve the manipulation of tools and utensils (Rancourt and Hogan 2001). For example, the action of an artist using a hammer and chisel to make a sculpture is inherently unstable. Small forces in the direction parallel to the surface of the material being sculpted can cause the chisel to slip. The chisel must be struck squarely with the head of the hammer or the resulting force may be misdirected and mar the artist's work. However, with practice, humans can acquire the skill to compensate for such unstable interactions.

The viscoelastic properties of muscle play an important role in motor control as they respond instantaneously to disturbances and stabilize movements. The greater the arm's viscoelastic impedance, the more it resists disturbances that perturb it away from its equilibrium position or intended trajectory. The ability to control viscoelastic impedance is particularly important for stabilizing movements in unstable environments (Burdet et al. 2001) or unpredictable situations (Takahashi et al. 2001).

Hogan (1985) hypothesized that impedance might be selectively controlled by the CNS, and we recently verified that hypothesis. We showed that the endpoint stiffness of the arm could be tuned to the direction of an instability (Burdet et al. 2001; Franklin et al. 2003a). Such selective change in stiffness orientation toward the direction of an instability is likely achieved by changes in the feedforward muscle activation, i.e., by controlling the activation level of particular muscle pairs. To investigate the sophistication of impedance control by the CNS, we varied the level of instability of a force field and measured the endpoint stiffness of the arm after adaptation. Based on our previous experiments, we expected a gradual increase in endpoint stiffness in the direction of the instability with little or no change in the perpendicular direction. We also anticipated that the net stiffness of the arm and the environment would remain constant if the CNS attempted to maintain a specific margin of limb stability while interacting with the environment. Such regulation of endpoint stiffness would produce a gradual elongation of the stiffness ellipse in the direction of the instability as the degree of instability increased.

METHODS

Subjects

Five healthy, right-handed subjects participated in the study (4 male and 1 female). The experiments were approved by the institutional ethics committee and subjects gave informed consent.

Address for reprint requests and other correspondence: D. W. Franklin, ATR Computational Neuroscience Laboratories, 2-2-2 Hikaridai, Keihanna Science City, Kyoto 619-0288, Japan (E-mail: dfrank@atr.jp).

The costs of publication of this article were defrayed in part by the payment of page charges. The article must therefore be hereby marked "advertisement" in accordance with 18 U.S.C. Section 1734 solely to indicate this fact.

Apparatus

Subjects were seated with their shoulders restrained against the back of a chair by a shoulder harness. A custom-molded rigid thermoplastic cuff was securely fastened around the subjects' right wrist and forearm, immobilizing the wrist joint. Only the shoulder and elbow joints remained free to move in the horizontal plane. The subjects' forearm was secured to a support beam in the horizontal plane, and the cuff and beam were coupled to the handle of the parallel-link direct drive air-magnet floating manipulandum (PFM). Movement was thus restricted to a single degree of freedom in each joint in the horizontal plane. Our coordinate system was positive to the right (x -axis) and forward (y -axis) relative to the shoulder.

The PFM was powered by two DC direct-drive motors controlled at 2 kHz, and the subjects' hand position was measured using optical joint position sensors (409,600 pulse/rev). The force applied by subjects at the handle of the PFM was measured using a six-axis force-torque sensor (Nitta Corp. no. 328) with a resolution of 0.06 N. The handle of the PFM (subjects' hand position) was supported by a frictionless air-magnet floating mechanism. The PFM was controlled by a digital signal processor (0.5 ms/cycle) to reduce the effect of the PFM's dynamics on the subjects' hand. Detailed descriptions of the PFM and controller have previously been published (Gomi and Kawato 1996, 1997).

The subjects' view of the PFM-cuff-forearm coupling was blocked by a table placed above the PFM. The start point, endpoint, and current hand position were displayed on the surface of the table with a projector mounted in the ceiling above the PFM. The start point and endpoint were, respectively, located 31 and 56 cm directly in front of the subjects' shoulder joint. A computer monitor placed behind the PFM displayed visual feedback information on the acceptance of a trial based on the timing and final location.

Procedure

Subjects produced point to point movements with their arm in a null field (NF) and in a position-dependent (divergent) force field (DF) of several different strengths. The divergent force fields added negative stiffness to the arm, causing a destabilizing or unstable interaction between the robotic interface and the subjects' arm. The DF produced negative elastic force perpendicular to the target direction. If the subject made a perfectly straight movement along the y -axis from start to endpoint, zero perpendicular force was produced. However, if the subject deviated from the y -axis, a perpendicular x -force was introduced, increasing with deviation. Noise due to variability in the descending motor command would normally cause the initial movement direction to vary from trial to trial. The DF had an amplifying effect on this motor output variability. Even relatively small deviations in the initial trajectory, to one side or the other, caused the arm to deviate farther and farther from the y -axis as the perpendicular force increased. The DF was implemented as

$$\begin{bmatrix} F_x \\ F_y \end{bmatrix} = \begin{bmatrix} \beta x \\ 0 \end{bmatrix} \quad (1)$$

where β (N/m) was chosen from the set {200, 300, 400, 500}. Values of β both larger and smaller than each subject's measured NF stiffness were used such that the interaction ranged from slight destabilization to instability. Only the two strongest subjects experienced the 500 strength force field. x is the lateral component of the subjects' hand position relative to the shoulder, and F_x and F_y are the forces generated by the PFM in the x - and y -directions, respectively. Each subject learned the force fields in a different order, and no two force field strengths were presented on a single day. Usually many days separated the presentation of two strengths of the force field. Previous work has shown that subjects are able to adapt to this unstable force field (Burdet et al. 2001; Franklin et al. 2003b; Osu et al. 2003). A

safety boundary (deviation of y -axis >0.05 m) was implemented beyond which the force field reverted to a NF.

The experiment had two parts for each force field: learning and stiffness estimation. The stiffness measurements were taken either on the same day as learning or 1 day after based on the availability of the equipment. In the learning phase, subjects first performed 20 successful movements in the NF. A successful trial was one in which movement terminated within the allocated time (0.6 ± 0.1 s) and within the 2.5-cm-diam end target. After 20 successful NF trials, the DF was activated, although the subjects were given no warning. Subjects then practiced in the force field until 100 successful trials had been completed. All trials were recorded whether they were successful or not.

After learning, the endpoint stiffness was measured using controlled displacements (Burdet et al. 2000, 2001; Franklin et al. 2003a). Subjects first completed 40 successful movements in the force field. Then an additional 160 trials were performed, 80 of which were randomly selected for stiffness estimation. For each of these 80 trials, the PFM was programmed to briefly displace the subjects' hand at the midpoint of the movement in one of eight randomly chosen directions. The PFM briefly perturbed the subjects' hand by a constant distance and then returned the hand to its predicted unperturbed trajectory. Full details of the stiffness estimation method appear elsewhere (Burdet et al. 2000).

Learning

To determine whether learning had occurred, hand-path error E , representing the area between the actual trajectory and the straight line joining the start and end targets, was calculated as in Osu et al. (2003). The calculation was performed from *time 0* (75 ms before hand-velocity crossed a threshold of 0.05 ms^{-1}) to *time T* (the termination time when curvature exceeded 0.07 m^{-1} ; Pollick and Ishimura 1996). Hand-path error was calculated for all practice trials. If the subjects' hand deviated from the y -axis by >0.05 m at any time during a particular trial, crossing the safety boundary, the x -axis position was considered to remain at 0.05 m for the rest of the trial. This method of calculation was used to ensure that the error was accurately represented even though the force field was shut off if subjects crossed the safety boundary. An ANOVA was performed to examine whether learning took place. The hand-path error on the first 10 and last 10 trials in the DF force fields was compared across all subjects (random effect) and field levels. A similar analysis was performed using the last 10 trials in the NF prior to the start of the DF and comparing them to the last 10 trials in the DF. This was done to compare performance at the end of practice to performance in the NF field.

Endpoint force of the arm was recorded during all of the experiments. After adaptation, the mean force applied to the hand should not have been different from that in the NF, regardless of the strength of the DF. To confirm this, an ANOVA was performed across all force field strengths, with subjects as a random effect, comparing the x - and y -forces in the 20 NF trials prior to the onset of the DF to the last 20 successful trials during practice in the DF. Time varying muscle torque at the shoulder and elbow was estimated using the equations of motion for a two-link planar arm. Full details appear elsewhere (Franklin et al. 2003b).

Stiffness estimation

The endpoint stiffness of the arm was measured after learning the NF as well as after learning in each DF. Full details of the method and analysis procedure are found elsewhere (Burdet et al. 2000; Franklin et al. 2003a). Basically, a ramp up/hold/ramp down servo-controlled displacement was applied to the hand near the midpoint of the movement. Using the average force and displacement during a 60-ms interval toward the end of the hold period, an estimate of the 2×2

endpoint stiffness matrix (**K**) was obtained by linear regression as represented by the equation

$$\begin{bmatrix} \Delta F_x \\ \Delta F_y \end{bmatrix} = \mathbf{K} \begin{bmatrix} \Delta x \\ \Delta y \end{bmatrix} = \begin{bmatrix} K_{xx} & K_{xy} \\ K_{yx} & K_{yy} \end{bmatrix} \begin{bmatrix} \Delta x \\ \Delta y \end{bmatrix} \quad (2)$$

where ΔF_x , ΔF_y , Δx , and Δy represent the mean change in endpoint force in the x- and y-directions and the mean change in displacement in the x- and y-directions, respectively. The stiffness in different directions was represented in terms of an ellipse by plotting the elastic force produced by a unit displacement (Mussa-Ivaldi et al. 1985). This was done using the singular value decomposition method (Gomi and Osu 1998).

The joint stiffness (**R**) was calculated from the endpoint stiffness (**K**) using the relation

$$\mathbf{R} = \begin{bmatrix} R_{ss} & R_{se} \\ R_{es} & R_{ee} \end{bmatrix} = \mathbf{J}^T \mathbf{K} \mathbf{J} - \frac{\partial \mathbf{J}^T}{\partial \theta} \mathbf{F} \quad (3)$$

where **J** represents the Jacobian transformation matrix from endpoint coordinates to joint coordinates, and the last term represents the change in endpoint force due purely to the change in the geometry of the arm produced by the displacement (Franklin and Milner 2003). The Jacobian and force matrices were fixed using the mean values for position and force during the measurement interval for each subject.

RESULTS

Changes in kinematics during practice

In the NF, subjects performed smooth accurate movements to the target (Fig. 1). Small variations in the duration and path occurred from trial to trial, likely due to factors such as motor noise (Clancy and Hogan 1995; Harris and Wolpert 1998;

Jones et al. 2002; Van Beers et al. 2004; van Galen and van Huygevoort 2000) and temporal deformation of the motor command (Morishige et al. 2004). However, these were insignificant compared with trajectory deviations produced when the DF was first activated. Subjects' movements were markedly perturbed either to the right or the left of their normal paths, and many crossed the safety boundary. This was true even for low levels of instability, which only marginally destabilized the interaction between the arm and the PFM. The destabilizing properties of the DF caused an amplification of the trial to trial variability seen in the NF. As learning progressed, subjects' performance improved and relatively straight movements to the target were achieved on most trials. They were able to adapt the control of their arm to counteract the destabilizing effect of the DF. By the end of the training period, the trajectories were relatively straight and generally successfully reached the end target, similar to NF trials. Subjects required an average of 114 ± 10 trials to achieve 100 successful trials.

The hand-path error was calculated for all levels of instability (NF and DF). Early trials in the DF had large hand-path errors, but these were gradually reduced during practice (Fig. 2). An ANOVA was performed to examine whether performance improved. The hand-path error on the first 10 trials and the last 10 trials in the DF (learning) was compared across all subjects (random effect) and field strength. A significant main effect of practice was found ($F = 9.754, P = 0.029$), indicating that subjects were able to significantly reduce their hand-path error by the end of practice in all fields. A significant interaction effect between practice and field strength was also found ($F = 4.053, P = 0.045$), indicating that the different force field strengths caused different amounts of error in subjects' movements. This likely arises because the different field strengths would amplify the variability in the trajectories to different degrees, causing the magnitude of the error at the beginning of practice to depend of the strength of the force field. To confirm this, the hand-path error for the first 10 trials in the force fields was compared using an ANOVA (Fig. 2D). The field strength had a significant effect on the size of the error ($F = 3.031, P = 0.031$). Further support was provided by Scheffe's post hoc multiple comparison test, which indicated that the hand-path error in the lowest and highest strength fields was significantly different. However, in all cases, subjects adapted to the changed dynamics, and the hand-path error values were reduced. Not surprisingly, the success rate paralleled the hand-path error. When the hand-path error was large, the success rate was low. The relatively low initial success rate at the highest force field strength is similar to that found by Milner (2002b), who investigated the ability of subjects to maintain a stable posture in the DF. As subjects adapted to the force field and reduced the hand-path error, the success rate also improved, particularly for the highest force field strength.

To determine the extent to which the errors were reduced, the first 10 NF trials before the activation of the DF and the last 10 practice trials in the DF were examined using an ANOVA with main effect of field strength and with subjects as a random effect. No significant difference was found between NF and DF hand-path errors ($F = 2.365, P = 0.197$). This result indicates that hand-path error in the DFs was reduced to a level similar to hand-path error in the NF by the end of practice. Furthermore, no effect of field strength was found ($F = 1.974, P =$

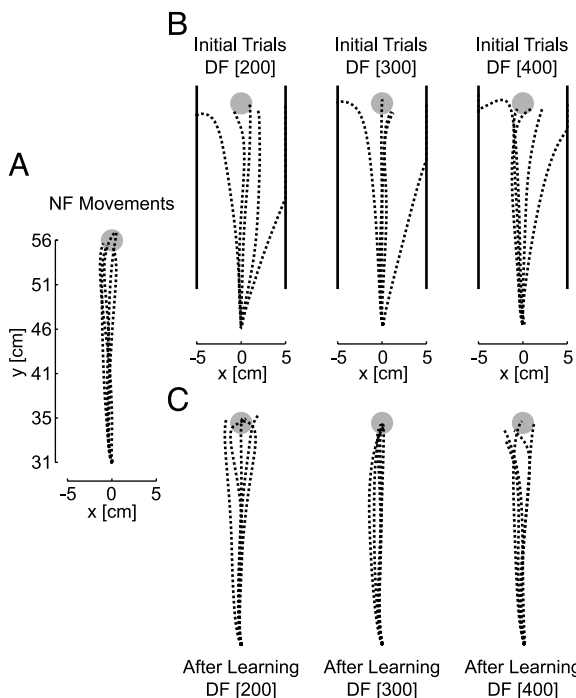


FIG. 1. Unstable force field initially amplifies the variability of trajectories. A: movements in the null field (NF). B: initial 5 trials in the position-dependent force field (DF). The safety boundary is shown by solid black lines to either side of the trajectories, outside of which the force field was inactivated for safety reasons. C: final 5 movements in the DF. Force fields for this subject were 200, 300, and 400 N/m.

0.189), suggesting that error was reduced to levels similar to that in the NF for all force field strengths. This indicates that subjects were able to stabilize movements and achieve movement trajectories similar to those in a stable, free environment by the end of practice across all levels of instability.

Endpoint forces after practice

At the beginning of the learning session in the DF, subjects experienced relatively large forces in the *x*-direction, which

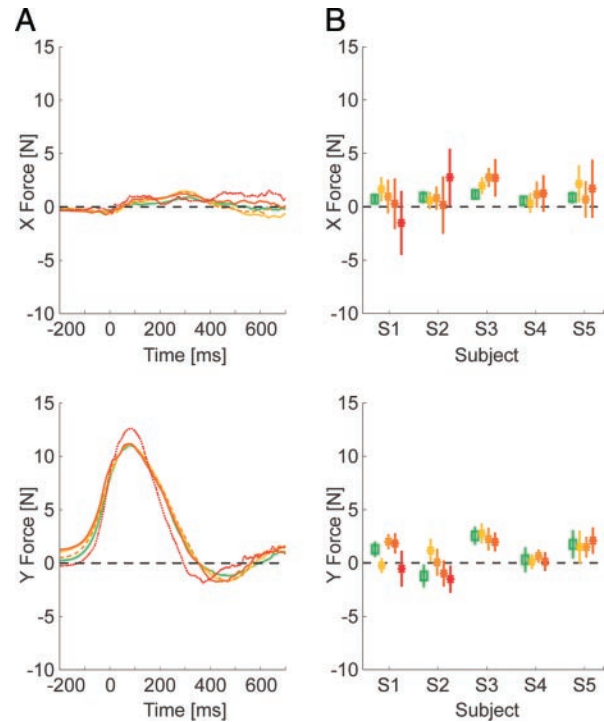
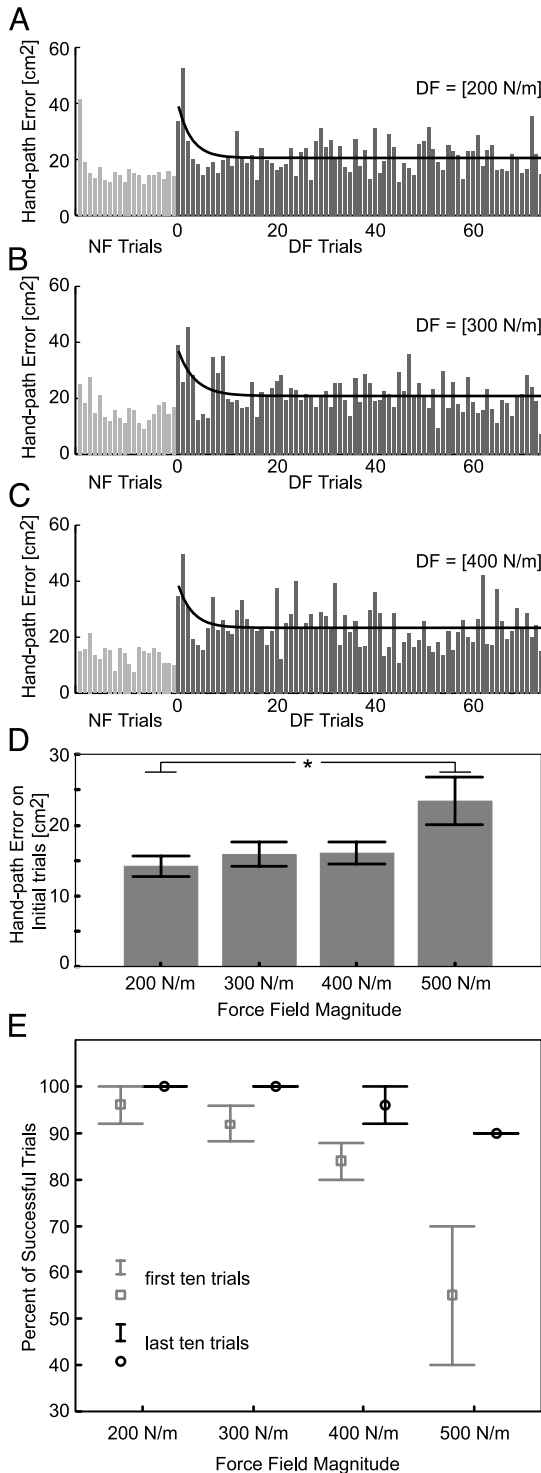


FIG. 3. Endpoint forces were similar across all force field strengths after learning. *A*: mean endpoint force profiles for the *x*- (*top*) and *y*-axes (*bottom*) during movements after learning in the NF (green), 200 DF (yellow), 300 DF (light orange dashed), 400 DF (dark orange), and 500 DF (red dotted). Only subjects 1 and 2 performed trials in the 500 DF. *B*: mean and SD *x*- (*top*) and *y*-force (*bottom*) at the midpoint of movements after adaptation for all force fields. The midpoint of movements refers to the time at which stiffness was estimated.

were positive or negative, depending on the initial direction of the trajectory. Once adaptation had occurred, and subjects were able to make relatively straight movements, the *x*- and *y*-forces measured in the DF did not differ significantly from those in the NF (Fig. 3). An ANOVA compared the *x*- and *y*-forces in the 20 NF trials prior to activation of the DF to the corresponding forces in the last 20 successful trials of practice in the DF (practice main effect), across all levels of instability (field strength effect) with subjects as a random effect. The results from the ANOVA found no significant differences for the forces in the DF compared with the forces in the NF for either the *x*- or *y*-directions ($F = 1.639$, $P = 0.266$ and $F = 6.010$, $P = 0.067$, respectively). Similarly, no effect was found for level of instability in either the *x*- or *y*-force directions ($F = 1.898$, $P = 0.200$ and $F = 0.493$, $P = 0.696$, respectively).

FIG. 2. Hand-path error is reduced during adaptation to the DF. *A*–*C*: error in the NF for 20 trials prior to the onset of the DF, and 70 practice trials in the DF are plotted for the 200-, 300-, and 400-N/m fields. Values shown are the average of all 5 subjects. Early trials in the DF have large errors, but these were reduced quickly as subjects adapted to the environmental dynamics. *D*: initial hand-path error (over 1st 10 movements) increased as the field strength increased. Hand-path error in the strongest field was significantly different from that in the weakest field ($P = 0.03$). The black line indicates the exponential best fit to the data as described previously (Osu et al. 2003). *E*: success rate in DF. Percent of successful trials (not exiting the safety boundary) is shown for the 1st (red) and last (blue) 10 learning trials at each field strength. Error bars represent SE. Success rate in the early trials depended on the field strength ($F = 8.282$, $P = 0.002$), where the 500 field was significantly less than the 200 and 300 fields (Scheffe's post hoc test). After learning, the success rate on the last 10 trials was not significantly different across any of the force fields ($F = 2.517$, $P = 0.104$).

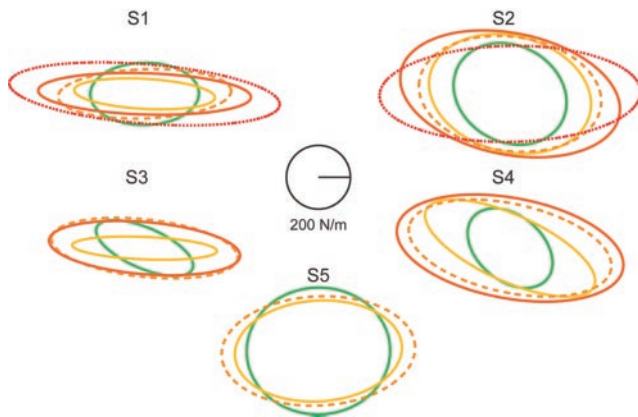


FIG. 4. Endpoint stiffness scales with strength of the unstable force field. Endpoint stiffness ellipses after adaptation are shown for all 5 subjects in the NF (green line), 200 DF (yellow line), 300 DF (light orange dashed line), 400 DF (dark orange line), and 500 DF (red dotted line).

Even for different levels of instability, the mean forces produced by subjects remained similar to those in the NF once learning had taken place. Variance in endpoint force in the DF was greater than in the NF because similar trial-to-trial variation in path was accompanied by larger forces in the DF than in the NF. Nevertheless, adaptation to the DF required no change in mean endpoint force compared with the NF.

Endpoint stiffness

After adaptation to each force field, each subjects' endpoint stiffness was measured at the midpoint of the movement during movements in the force field (Fig. 4). Compared with the NF stiffness ellipses, the DF stiffness ellipses were more anisotropic or elongated. In particular, the dimension of the stiffness ellipses remained similar to those in the NF for the y -direction, whereas in the x -direction, the dimension of the stiffness ellipses increased as field strength (level of instability) increased. Although endpoint forces remained unchanged, subjects were able to modify their endpoint stiffness, indicating that the CNS was controlling stiffness via impedance control rather than as a side effect of changes in endpoint force (Burdet et al. 2001; Franklin et al. 2003a). This specific scaling of stiffness in the x -direction (direction of instability) with level of instability indicates that stability was not achieved by simply co-contracting all the muscles of the arm equally. If subjects had adapted to a force field by using such generalized muscle co-contraction, the resulting stiffness ellipse would have been modified mainly in size rather than in orientation and shape.

When the experiments were initially conducted with two of the subjects (S3 and S4), the stiffness ellipses were found to have increased in both the x - and y -directions after adaptation to several levels of the force field. This differed from the results for the other subjects and for the results of previous experiments (Burdet et al. 2001; Franklin et al. 2003a). We hypothesized that these subjects were either unable to control stiffness independently along the two directions unlike other subjects or they required more training to learn the adaptation strategy used by the other subjects. To test these hypotheses, we had the subjects perform an additional practice session followed by stiffness measurement for each force field. Subjects performed another 200 practice trials, and stiffness was

again measured. These subjects therefore had practiced ≥ 500 trials in the force field altogether before the second stiffness measurement. The stiffness measurements before and after the second practice session are compared in Fig. 5. After more extensive practice, the endpoint stiffness was smaller in both the x - and y -directions than measurements made earlier ($P = 0.004$ and $P = 0.011$, respectively). The reduction [(original K - new K)/original K] along the x -axis was small (12.6%) compared with the reduction along the y -axis (49.4%).

To further investigate the effect of the level of instability (field strength) on the endpoint stiffness of the limb, the x - and y - (diagonal) components of the stiffness matrix \mathbf{K} for each subject and field strength were examined (Fig. 6). The x -stiffness in the DF increased progressively with level of DF instability. An ANOVA was performed on the x -component of stiffness for field strength, with the NF being classified as 0. A highly significant effect was found ($F = 35.015$, $P < 0.001$), supporting this observation. In contrast, no significant differences (ANOVA) in stiffness in the y -direction were found with level of instability ($F = 0.362$, $P = 0.832$). Further support was provided by Scheffe's post hoc multiple comparison test, performed on the y -component of stiffness for each field strength, which showed no significant differences between any two levels and found only one homogenous subset. The same test performed on the x -component of stiffness found four homogenous subsets at a significance level of $\alpha = 0.05$. This means that the x -component of stiffness was selectively increased as field strength was increased without significantly changing the y -component of stiffness.

The net stiffness is a representation of the combined stiffness of the arm and the environment in the x -direction and is calculated as the difference between the measured arm stiffness and the force field stiffness. The net stiffness determines the overall stability of the interaction between the arm and the environment. For each force field strength, the net stiffness required to stabilize movements remained constant, at a level similar to the NF (Fig. 6A, black). An ANOVA performed on the net stiffness in each field across all force levels and subjects indicated no significant difference ($F = 2.176$, $P = 0.129$). A post hoc test also found only one homogenous subset and confirmed that there was no significant difference between net stiffness for any two field strengths, including the NF. The

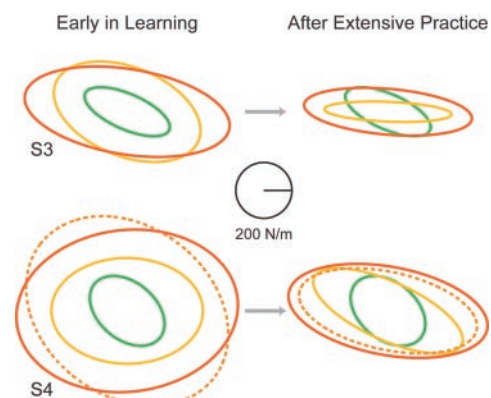


FIG. 5. Endpoint stiffness reduced in y -direction with sufficient training. Endpoint stiffness ellipses are shown for 2 subjects after the initial learning session (left) and after further training on a subsequent day (right). Ellipses are shown using the same color code as in Fig. 3. NF ellipses are also shown for comparison.

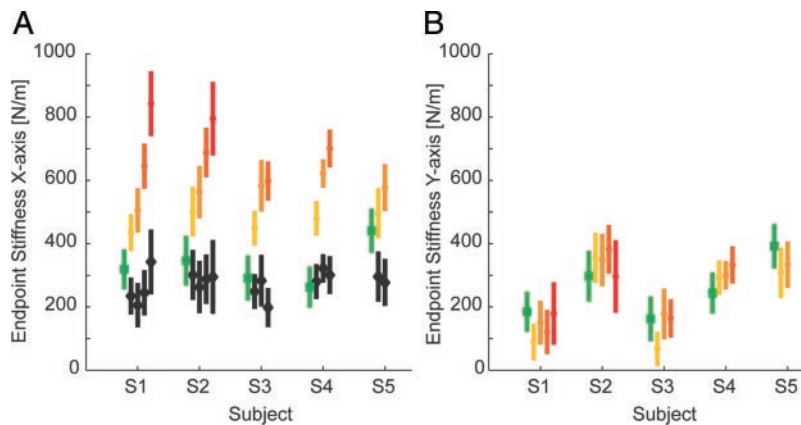


FIG. 6. The x - and y -components of endpoint stiffness together with the net stiffness of the interaction between the limb and the force field. *A*: the x -component of endpoint stiffness after adaptation for all subjects in the NF (green), 200 DF (yellow), 300 DF (light orange), 400 DF (dark orange), and 500 DF (red). The net stiffness (stiffness of the interaction between the limb and DF) after learning is shown in black. Vertical bars show 90% CIs. *B*: the y -component of endpoint stiffness in the same force fields.

results indicate that in adapting to the unstable dynamics of this study, the impedance controller selectively increased stiffness in the direction of instability while maintaining stiffness in the stable direction at a level similar to that in the NF. The arm stiffness in the unstable direction was modified in a manner such that net stiffness remained at a level similar to that in the NF. This indicates that the CNS attempted to maintain a specific level of stability when adapting to unstable dynamics of different strengths.

Joint stiffness

The joint stiffness was estimated from the measurements of endpoint stiffness. The shoulder and elbow joint stiffness (R_{ss} , R_{ee}) values were plotted against shoulder and elbow joint torque, respectively, for all subjects at all force field strengths (Fig. 7). A linear regression was performed, and no significant correlation was found between shoulder joint stiffness and shoulder joint torque ($r^2 = 0.002$). Similarly, no significant relationships were found for either of the cross-joint stiffness terms with either elbow or shoulder joint torque. The elbow joint stiffness was correlated with the elbow joint torque ($r^2 = 0.32$). However, the slope of this relation was much greater than that found in previous studies under isometric conditions (Franklin and Milner 2003; Gomi and Osu 1998).

DISCUSSION

We have investigated the adaptation of limb impedance to different levels of instability perpendicular to the direction of movement. These destabilizing force fields initially caused the subjects' trajectories to deviate to either side of the straight line between start and end targets. With sufficient practice, the subjects were able to adapt to the force fields and perform movements to the target similar to those in the null force field. After adaptation, there was little difference between the forces applied to the hand for any of the force fields compared with the null force field. Therefore any changes in the stiffness were not produced simply by a change in the joint torque. The endpoint stiffness of the limb increased with the strength of the force field. In particular, the stiffness in the x -direction increased in proportion to the increasing instability of the force field, which was oriented in that direction, whereas the stiffness in the y -direction did not significantly change with the strength of the force field. The overall stiffness in the x -direction, encompassing the stiffness of the limb and that of the environ-

ment (net stiffness), was maintained at a constant level across all force field strengths.

Interaction between motor noise and instability

When we make repeated movements, there are small variations in the trajectories from trial to trial. These trajectory variations are produced by factors such as motor noise (Clancy and Hogan 1995; Harris and Wolpert 1998; Jones et al. 2002;

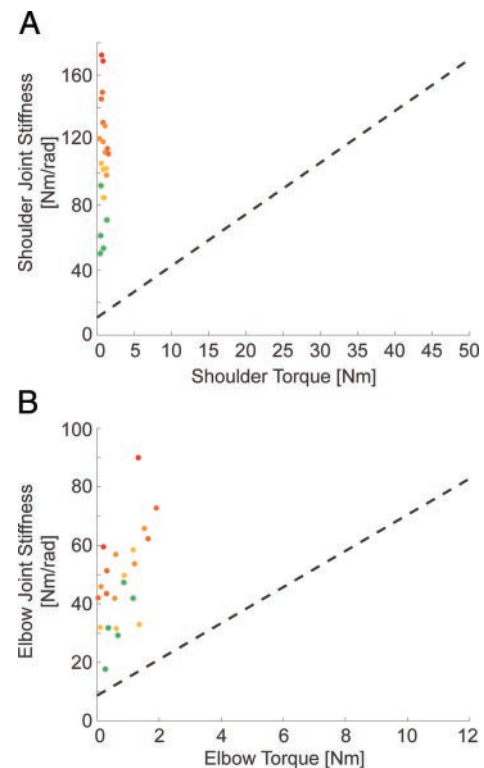


FIG. 7. Joint stiffness increases independently of joint torque for adaptation to unstable dynamics. *A*: shoulder joint stiffness R_{ss} plotted against shoulder joint torque τ_s for all subjects in all force fields. Color of the dots indicates from which force field the measurement came, using the same color scheme as the previous figures. Dashed line was produced using the mean slope and intercept data from the work of Gomi and Osu (1998). Line represents relationship between shoulder joint stiffness and shoulder torque found during stable posture ($R_{ss} = 3.18 \times \tau_s + 10.80$). *B*: elbow joint stiffness R_{ee} plotted against τ_e for all subjects in all force fields. Dashed line again represents relationship between elbow joint stiffness and elbow torque from Gomi and Osu (1998) ($R_{ee} = 6.18 \times \tau_e + 8.67$).

Van Beers et al. 2004; van Galen and van Huygevoort 2000) and temporal deformation of the motor command (Morishige et al. 2004). These variations may generally be small enough not to interfere with the performance of most activities. For movements in an unstable environment, however, the effect of motor noise is critical. The variability in trajectory produced by the motor noise is amplified by the instability of the force field. This produces a diverging trajectory to either one side or the other of the desired path. To compensate for this effect, the CNS must counteract the instability of the force field by increasing the stability of the limb or by reducing the variability to zero. It seems that eliminating the motor noise is not an option, so instead, the CNS increases the stiffness of the limbs to stabilize the total system of the limb and its environment. This is similar to the strategy used to achieve higher accuracy for a given movement speed or to achieve the same accuracy for faster movements (Grey 1997; Gribble et al. 2003; Osu et al. 2004).

Stiffness change is independent of joint torque

As muscles are activated, the stiffness increases along with the increasing muscle force (Kirsch et al. 1994). This translates into an increase in joint stiffness with increasing joint torque (Carter et al. 1990; Gottlieb and Agarwal 1988; Hunter and Kearney 1982; Milner et al. 1995; Weiss et al. 1988). Similarly, the joint stiffness terms have been found to increase linearly with the joint torque under stable conditions for a multi-joint limb (Gomi and Osu 1998; Perreault et al. 2001, 2002). This is in sharp contrast to the results reported here, where the joint stiffness increased with little change in the joint torques. Although the stiffness of the elbow joint was correlated with the joint torque, the slope of the relationship showed that only a small portion of the change in stiffness could have been produced by the change in torque. By co-contracting antagonist muscles, the joint stiffness can be increased without changing the net joint torques (Hogan 1984). This increased co-contraction and joint stiffness allows the limb to counteract the instability in the environment such that unperturbed movements are possible (De Serres and Milner 1991; Milner 2002a).

Our previous work, examining this adaptation to unstable dynamics carefully, modeled the changes in force and stiffness on a trial by trial basis and found that the change in stiffness could not be explained by the direct relationship between the changes in muscle stiffness and muscle force (Franklin et al. 2003a). However, as only a single field strength was examined, the variation in joint stiffness was relatively small. Consequently, it was not possible to correlate joint stiffness with joint torque. In this experiment, there was a large variation in joint stiffness but we found almost no correlation between joint stiffness and joint torque, confirming that the stiffness change was controlled independently of joint torque. This supports our hypothesis that the CNS explicitly controls the impedance of the limb by learning an internal model related to the stability of the external environment (Osu et al. 2003; Franklin et al. 2003b).

Net stiffness of the interaction is regulated

The net stiffness is the combined stiffness of the environment and the limb. In our case, it represents the stability of the

interaction between the man and machine. Burdet et al. (2001) found that the net stiffness after adaptation was positive, indicating a stable interaction, and that it was similar to the limb stiffness in the null force field. In this experiment, the net stiffness of the combined arm and environment was found not to vary with the level of instability. This has important ramifications for the understanding of motor control. The neuromuscular system must be able to judge the instability of the environment and adapt the stiffness of the limb to maintain this constant net stiffness. The idea that we are able to judge the stiffness of the environment is not new, other researchers have found evidence that humans are able to judge their environmental impedance (Jones and Hunter 1990, 1993). This may occur through the estimation of both changes in environmental force and its effect on limb kinematics. However, when moving, kinematic error alone may be sufficient to learn to counteract the effect of instability in the environment. We propose that the CNS uses the kinematic error on a given trial to update an impedance model of the environment for modifying feedforward motor commands for the next trial. Using error information from movements during repeated trials, we can slowly build up an internal representation of the stability of a task performed in a specific environment or with a specific tool and compensate for any instability. Such changes in the feedforward control would be intimately related to the development of an inverse dynamics model to compensate for necessary changes in the external force (Franklin et al. 2003a).

Control of the endpoint stiffness characteristics

This study confirms the findings of our previous work (Burdet et al. 2001; Franklin et al. 2003a) and generalizes them for different levels of instability. In particular, we were able to show that the stiffness of the limb is not just selectively increased in the direction of the instability but that it increases in proportion to the level of instability. This provides clear evidence that the CNS is able to control the impedance of the limb as proposed by Hogan (1985).

Studies of multi-joint impedance under static conditions have generally found limited control over the orientation and shape of the stiffness ellipse (Gomi and Osu 1998; Perreault et al. 2002). However, in these studies, subjects were instructed to modulate their stiffness based on the feedback of EMG or measured endpoint stiffness. In contrast, during movement in an unstable environment, we have shown that the stiffness of the limb can be rotated and elongated selectively in the direction of the instability. The question remains whether this is particular to movement as opposed to posture or whether it occurs as a result of the feedback and learning signals, which are used to guide the subjects. In our experiment, subjects must increase the impedance of the limb above that of the environment to succeed at the task. They are also required to practice extensively. They, therefore, receive two key signals which may allow the CNS to learn this control of the endpoint stiffness. The first is proprioceptive sensory information from the periphery, which can be used to evaluate the instability of the environment. The second is the cumulative effect of co-contraction. High levels of co-contraction allow subjects to succeed at the task but can also lead to fatigue. Subjects performing the task only once may increase stiffness far above the minimum that is required. However, subjects performing

the task repeatedly will find it useful to learn to minimize muscle activity. This view is supported by the finding that there was less co-contraction during a force control task than during a less stable position control task (Franklin and Milner 2003).

However, there are other possible explanations that could account for differences in impedance control between posture and movement. In recent experiments examining load sensitivity of neurons in primary cortex, it appears that independent populations of neurons respond to loads during posture (static loading) and movement (dynamic loading) (Scott 2004). Different excitatory and inhibitory projections of two such populations of cortical-motor neurons might result in differences in the ability to regulate co-contraction and stiffness. Nevertheless, there are theoretical limits to the modification of stiffness geometry by the CNS, and we are currently investigating how the CNS works within these constraints when the interaction dynamics are unstable.

Metabolic cost is reduced

To adapt to the DF, the CNS selectively modified stiffness such that a specific level of stability was maintained in the direction of the instability without change in the perpendicular direction. Under static conditions without training, Mussa-Ivaldi et al. (1985) found a global increase in stiffness in response to sinusoidal perturbations applied in specific directions. The strategy seen here, however, to maintain a specific stability margin for all levels of force field instability, was energy efficient, because any additional stiffness in either the stable or unstable directions would have required more muscle co-activation and thus more expenditure of metabolic energy. Increased muscle activity is generally related to increased metabolic cost (Foley and Meyer 1993; Hogan et al. 1996; Sih and Stuhmiller 2003). A nonspecific increase in stiffness magnitude would require co-activation of all pairs of antagonist muscles in the arm, which would be more costly in terms of energy expenditure than selective co-activation. The selective increase in stiffness along the direction of instability indicates that the CNS does not increase the activation of all muscles equally, but attempts to find a balance when modifying arm impedance. It faces the optimization problem of maintaining stability while minimizing metabolic cost.

A greater reduction in the metabolic cost might be achieved by relying on feedback control, either reflexive or voluntary, rather than feedforward control. However, there are several problems with such a strategy. First, feedback correction operates with a significant delay. During this time, the arm would be pushed farther away from the desired trajectory by the force field and the force applied to the arm would increase. Not only would the error be large, but the force needed to correct the error would be difficult to estimate because of the instability. In addition, the metabolic cost of initial force production is higher than that required to maintain the force level (Russ et al. 2002). Consequently, a series of brief contractions, e.g., 250 ms, could have a higher metabolic cost than a single contraction of longer total duration (Hogan et al. 1998). Therefore it may be more efficient metabolically to co-contrast muscles continuously to produce a stable interaction with the environment throughout the entire movement rather than reciprocally activating muscles and reacting to perturbations after they occur. Furthermore, such feedforward control can ensure that perturbations

do not occur, which is a prerequisite for skilled tool use that could not be guaranteed if the CNS relied on delayed feedback control.

While this paper attempts to explain the results in terms of achieving stability with minimal metabolic cost, there are also other possible explanations why the muscle activity is being reduced. In particular, other parameters such as net muscle generated stress at a joint or a measure of the effort or the neural activity could easily replace our proposed metabolic cost. The current work cannot distinguish between any of these related possibilities. However, we feel that the assumption that the CNS balances stability and metabolic cost is the most intuitive interpretation and the most understandable in terms of the evolutionary pressures on the development of motor learning.

ACKNOWLEDGMENTS

We thank T. Yoshioka for assistance in running the experiments and Drs. R. Osu and E. Burdet for helpful discussions.

GRANTS

This work was supported by the National Institute of Information and Communications Technology of Japan, the Natural Sciences and Engineering Research Council of Canada, and the Human Frontier Science Program.

REFERENCES

- Burdet E, Osu R, Franklin DW, Milner TE, and Kawato M.** The central nervous system stabilizes unstable dynamics by learning optimal impedance. *Nature* 414: 446–449, 2001.
- Burdet E, Osu R, Franklin DW, Yoshioka T, Milner TE, and Kawato M.** A method for measuring endpoint stiffness during multi-joint arm movements. *J Biomech* 33: 1705–1709, 2000.
- Carter RR, Crago PE, and Keith MW.** Stiffness regulation by reflex action in the normal human hand. *J Neurophysiol* 64: 105–118, 1990.
- Clancy EA and Hogan N.** Multiple site electromyograph amplitude estimation. *IEEE Trans Biomed Eng* 42: 203–211, 1995.
- Conditt MA, Gandolfo F, and Mussa-Ivaldi FA.** The motor system does not learn the dynamics of the arm by rote memorization of past experience. *J Neurophysiol* 78: 554–560, 1997.
- De Serres SJ and Milner TE.** Wrist muscle activation patterns and stiffness associated with stable and unstable mechanical loads. *Exp Brain Res* 86: 451–458, 1991.
- Foley JM and Meyer RA.** Energy cost of twitch and tetanic contractions of rat muscle estimated in situ by gated ³¹P NMR. *NMR Biomed* 6: 32–38, 1993.
- Franklin DW, Burdet E, Osu R, Kawato M, and Milner TE.** Functional significance of stiffness in adaptation of multijoint arm movements to stable and unstable dynamics. *Exp Brain Res* 151: 145–157, 2003a.
- Franklin DW and Milner TE.** Adaptive control of stiffness to stabilize hand position with large loads. *Exp Brain Res* 152: 211–220, 2003.
- Franklin DW, Osu R, Burdet E, Kawato M, and Milner TE.** Adaptation to stable and unstable dynamics achieved by combined impedance control and inverse dynamics model. *J Neurophysiol* 90: 3270–3282, 2003b.
- Gomi H and Kawato M.** Equilibrium-point control hypothesis examined by measured arm stiffness during multijoint movement. *Science* 272: 117–120, 1996.
- Gomi H and Kawato M.** Human arm stiffness and equilibrium-point trajectory during multi-joint movement. *Biol Cybern* 76: 163–171, 1997.
- Gomi H and Osu R.** Task-dependent viscoelasticity of human multijoint arm and its spatial characteristics for interaction with environments. *J Neurosci* 18: 8965–8978, 1998.
- Gottlieb GL and Agarwal GC.** Compliance of single joints: elastic and plastic characteristics. *J Neurophysiol* 59: 937–951, 1988.
- Grey MJ.** *Viscoelasticity of the Human Wrist During the Stabilization Phase of a Targeted Movement* (MSc thesis). Burnaby, Canada: Simon Fraser Univ., 1997.
- Gribble PL, Mullin LI, Cothros N, and Mattar A.** Role of cocontraction in arm movement accuracy. *J Neurophysiol* 89: 2396–2405, 2003.

- Harris CM and Wolpert DM.** Signal-dependent noise determines motor planning. *Nature* 394: 780–784, 1998.
- Hogan MC, Ingham E, and Kurdak SS.** Contraction duration affects metabolic energy cost and fatigue in skeletal muscle. *Am J Physiol* 274: E397–E402, 1998.
- Hogan MC, Kurdak SS, and Arthur PG.** Effect of gradual reduction in O₂ delivery on intracellular homeostasis in contracting skeletal muscle. *J Appl Physiol* 80: 1313–1321, 1996.
- Hogan N.** Adaptive control of mechanical impedance by coactivation of antagonist muscles. *IEEE Trans Auto Control AC* 29: 681–690, 1984.
- Hogan N.** The mechanics of multi-joint posture and movement control. *Biol Cybern* 52: 315–331, 1985.
- Hunter IW and Kearney RE.** Dynamics of human ankle stiffness: variation with mean ankle torque. *J Biomech* 15: 747–752, 1982.
- Jones KE, Hamilton AF, and Wolpert DM.** Sources of signal-dependent noise during isometric force production. *J Neurophysiol* 88: 1533–1544, 2002.
- Jones LA and Hunter IW.** A perceptual analysis of stiffness. *Exp Brain Res* 79: 150–156, 1990.
- Jones LA and Hunter IW.** A perceptual analysis of viscosity. *Exp Brain Res* 94: 343–351, 1993.
- Kawato M.** Internal models for motor control and trajectory planning. *Curr Opin Neurobiol* 9: 718–727, 1999.
- Kirsch RF, Boskov D, and Rymer WZ.** Muscle stiffness during transient and continuous movements of cat muscle: perturbation characteristics and physiological relevance. *IEEE Trans Biomed Eng* 41: 758–770, 1994.
- Krakauer JW, Ghilardi MF, and Ghez C.** Independent learning of internal models for kinematic and dynamic control of reaching. *Nat Neurosci* 2: 1026–1031, 1999.
- Lackner JR and Dizio P.** Rapid adaptation to Coriolis force perturbations of arm trajectory. *J Neurophysiol* 72: 299–313, 1994.
- Milner TE.** Adaptation to destabilizing dynamics by means of muscle cocontraction. *Exp Brain Res* 143: 406–416, 2002a.
- Milner TE.** Contribution of geometry and joint stiffness to mechanical stability of the human arm. *Exp Brain Res* 143: 515–519, 2002b.
- Milner TE, Cloutier C, Leger AB, and Franklin DW.** Inability to activate muscles maximally during cocontraction and the effect on joint stiffness. *Exp Brain Res* 107: 293–305, 1995.
- Morishige K, Miyamoto H, Osu R, and Kawato M.** Positional variance on via-point reaching movement supports sequential trajectory planning and execution model. *IEICE Trans Inf Syst* J87-D-II: 716–725, 2004.
- Mussa-Ivaldi FA, Hogan N, and Bizzi E.** Neural, mechanical, and geometric factors subserving arm posture in humans. *J Neurosci* 5: 2732–2743, 1985.
- Osu R, Burdet E, Franklin DW, Milner TE, and Kawato M.** Different mechanisms involved in adaptation to stable and unstable dynamics. *J Neurophysiol* 90: 3255–3269, 2003.
- Osu R, Kamimura N, Iwasaki H, Nakano E, Harris CM, Wada Y, and Kawato M.** Optimal impedance control for task achievement in the presence of signal-dependent noise. *J Neurophysiol* 92: 1199–1215, 2004.
- Perreault EJ, Kirsch RF, and Crago PE.** Effects of voluntary force generation on the elastic components of endpoint stiffness. *Exp Brain Res* 141: 312–323, 2001.
- Perreault EJ, Kirsch RF, and Crago PE.** Voluntary control of static endpoint stiffness during force regulation tasks. *J Neurophysiol* 87: 2808–2816, 2002.
- Pollick FE and Ishimura G.** The three-dimensional curvature of straight-ahead movements. *J Motor Behav* 28: 271–279, 1996.
- Rancourt D and Hogan N.** Stability in force-production tasks. *J Motor Behav* 33: 193–204, 2001.
- Russ DW, Elliott MA, Vandenborne K, Walter GA, and Binder-Macleod SA.** Metabolic costs of isometric force generation and maintenance of human skeletal muscle. *Am J Physiol* 282: E448–E457, 2002.
- Scott SH.** Neural correlates of limb mechanics and mechanical loads in primary motor cortex. In: *Proceedings of the 31st NIPS International Symposium*, Okazaki, Japan: NIPS, 2004, p. 36.
- Shadmehr R and Mussa-Ivaldi FA.** Adaptive representation of dynamics during learning of a motor task. *J Neurosci* 14: 3208–3224, 1994.
- Sih BL and Stuhmiller JH.** The metabolic cost of force generation. *Med Sci Sports Exerc* 35: 623–629, 2003.
- Takahashi CD, Scheidt RA, and Reinkensmeyer DJ.** Impedance control and internal model formation when reaching in a randomly varying dynamical environment. *J Neurophysiol* 86: 1047–1051, 2001.
- Van Beers RJ, Haggard P, and Wolpert DM.** The role of execution noise in movement variability. *J Neurophysiol* 91: 1050–1063, 2004.
- van Galen GP and van Huygevoort M.** Error, stress and the role of neuromotor noise in space oriented behaviour. *Biol Psychol* 51: 151–171, 2000.
- Weiss PL, Hunter IW, and Kearney RE.** Human ankle joint stiffness over the full range of muscle activation levels. *J Biomech* 21: 539–544, 1988.